Biochemical Pharmacology 80 (2010) 1736–1745

Contents lists available at ScienceDirect

Biochemical Pharmacology

journal homepage: www.elsevier.com/locate/biochempharm

Mechanisms of metformin action on glucose transport and metabolism in human adipocytes

Jean Grisouard [a,*], Katharina Timper [a], Tanja M. Radimerski [a], Daniel M. Frey [b], Ralph Peterli [c], Blerina Kola [d], Márta Korbonits [d], Paul Herrmann [e], Stephan Krähenbühl [f], Henryk Zulewski [a], Ulrich Keller [a], Beat Müller [g], Mirjam Christ-Crain [a]

[a] Department of Biomedicine, Metabolism Group, Div. of Endocrinology, Diabetes and Clinical Nutrition, University Hospital Basel, CH-4031 Basel, Switzerland
[b] Department of Surgery, Div. of General Surgery and Surgical Research, University Hospital Basel, CH-4031 Basel, Switzerland
[c] Department of Surgery, Claraspital Basel, CH-4016 Basel, Switzerland
[d] Department of Endocrinology, Barts and the London Medical School, Queen Mary, University of London, EC1M 6BQ London, UK
[e] Department of Pathology and Human Anatomy, Loma Linda University School of Medicine, Loma Linda, CA 92354, USA
[f] Department of Biomedicine, Clinical Pharmacology Group, University Hospital Basel, CH-4031 Basel, Switzerland
[g] Department of Internal Medicine, Kantonsspital Aarau, CH-5001 Aarau, Switzerland

ARTICLE INFO

Article history:
Received 7 July 2010
Accepted 25 August 2010

Keywords:
Glucose uptake
Glucose oxidation
Metformin
AMPKα1
GLUT-4
Human adipocytes

ABSTRACT

The mechanisms of metformin effects on glucose transport and metabolism were investigated in human adipocytes. Human preadipocytes obtained from surgical biopsies were differentiated in vitro into adipocytes and the effects of metformin on glucose uptake, glucose oxidation and the involved signaling pathways were analyzed. Metformin (1 mM, 24 h) increased glucose uptake 2.3 ± 0.2-fold ($p < 0.001$ vs. basal) in human adipocytes, without altering cell viability and oxygen consumption. Metformin did not alter GLUT-1 mRNA expression and protein content but increased GLUT-4 mRNA expression and cellular protein content, leading to increased GLUT-4 protein content in the plasma membrane. Neither basal nor insulin-induced phosphorylation of Akt at Ser-473 and AS160 (Akt substrate of 160 kDa) at Thr-642 were enhanced by metformin. Suppression of metformin-induced AMP-activated protein kinase (AMPK) activity by AMPKα1 silencing, however, reduced metformin-associated GLUT-4 expression and stimulation of glucose uptake. In addition, metformin induced glucose oxidation. In conclusion, activation of AMPKα1 without impairment of cell respiration is crucial for metformin-mediated increase in GLUT-4 protein content and glucose uptake in human adipocytes.

1. Introduction

Metformin, the most frequently used antidiabetic drug worldwide, improves peripheral glucose uptake and reduces hepatic glucose in patients with type 2 diabetes mellitus (T2DM). Metformin is used as monotherapy or in combination with other antidiabetic agents including insulin [1,2]. AMP-activated protein kinase (AMPK) is a regulator of cellular and systemic energy homeostasis and the activation of this enzyme by metformin provides an explanation for the beneficial effects of this drug in inhibiting glucose output from hepatocytes and in inducing glucose uptake in myocytes [3,4].

GLUT-1 and GLUT-4, the two main glucose transporter isoforms expressed in adipose tissue, mediate glucose uptake. GLUT-1 is located predominantly in the plasma membrane. In the basal state, GLUT-4 is stored in storage vesicles but upon insulin stimulation it is translocated to the plasma membrane, inducing glucose uptake [5]. Insulin triggers GLUT-4 translocation by incompletely defined complex intracellular signaling pathways that include the classical phosphatidylinositol 3′ kinase (PI3K)/Akt/AS160 pathway [6].

Recently, we reported that metformin induces glucose uptake in human preadipocyte-derived adipocytes from obese and non-obese patients [7]. In the present study, we investigated the mechanisms of metformin action on the Akt signaling pathway, glucose transporters and glucose uptake, as well as its effect on cell viability, cell respiration and glucose oxidation in these human adipocytes.

* Corresponding author at: University Hospital Basel, Department of Biomedicine, Metabolism Group (319), Hebelstrasse, 20, CH-4031 Basel, Switzerland. Tel.: +41 61 265 23 60; fax: +41 61 265 23 50.
E-mail addresses: jean.grisouard@unibas.ch (J. Grisouard), katharina.timper@yahoo.de (K. Timper), tanja.radimerski@unibas.ch (T.M. Radimerski), dfrey@uhbs.ch (D.M. Frey), Ralph.Peterli@claraspital.ch (R. Peterli), b.kola@qmul.ac.uk (s.$. Kola), m.korbonits@qmul.ac.uk (M. Korbonits), PHerrmann@llu.edu (P. Herrmann), kraehenbuehl@uhbs.ch (S. Krähenbühl), henryk.zulewski@unibas.ch (H. Zulewski), ulrich.keller@unibas.ch (s.$. Keller), happy.mueller@unibas.ch (B. Müller), Mirjam.Christ-Crain@unibas.ch (M. Christ-Crain).

0006-2952/$ – see front matter © 2010 Elsevier Inc. All rights reserved.
doi:10.1016/j.bcp.2010.08.021

2. Materials and methods

2.1. Cell culture and treatment

The study was approved by the local Ethics Committee. Subcutaneous fat tissue samples were obtained from 12 non-diabetic, six non-obese (five males, one female; aged 64 ± 6 years; BMI 22.5 ± 0.8 kg/m^2) and six obese (two males, four females; aged 50 ± 8 years; BMI 32.8 ± 1.5 kg/m^2) patients undergoing abdominal surgery. Mature isolated adipocytes (floating cells) were directly used, whereas the stromal-vascular cell fraction containing pre-adipocytes was isolated and the preadipocytes were expanded in vitro in DMEM (Lonza, Verviers, Belgium) containing 10% FCS and 5 ng/ml 2-FGF (Lubio Science, Luzern, Switzerland) until confluence, and subjected to adipogenic differentiation medium for 14 days, as previously described [7].

After differentiation, adipocytes were washed twice with PBS and kept for 48 h in low-glucose (5 mM) medium: DMEM supplemented with nutrient mixture F-12 (1.8 g/l glucose), L-ascorbic acid (100 nM), biotin (8 μg/ml), D-pantothenate (15 mM, Sigma–Aldrich, Buchs, Switzerland), gentamycin (50 μg/ml), HEPES (15 nM) and 3% FCS (Lubio Science). Adipocytes were then left untreated or treated with metformin (from 0.001 to 10 mM, Sigma–Aldrich) for 24 h, followed by stimulation with phloretin (50 μM, Sigma–Aldrich) and/or insulin (100 nM, Actrapid, Novo-Nordisk Pharma, Küsnacht, Switzerland) for 20 min.

2.2. Assessment of cell viability using flow cytometry

After treatment, preadipocyte-derived adipocytes were incubated with 2 μg/ml BODIPY™ 493/503 (Lubio Science) diluted in PBS for 20 min at room temperature (RT), washed with PBS and harvested with 0.5 g/l EDTA (Sigma–Aldrich) diluted in PBS. Cells were resuspended in PBS + 0.5% BSA (Sigma–Aldrich) and propidium iodide (PI) (Lubio Science) was added to yield a final concentration of 4 ng/ml. Cells were analyzed by flow cytometry (Beckman Coulter's CYAN™ Flow Cytometer, Allschwil, Switzerland) using Summit 4.3 software (Beckman Coulter). A 488-nm Laser was used for excitation and emission was collected at 530/40 nm for BODIPY™ and at 613/20 nm for PI.

2.3. Oxygen consumption rate

Preadipocytes were cultured and if necessary differentiated in XF24 Seahorse Bioscience cell culture plates (Bucher Biotec AG, Basel, Switzerland). After 48 h in low-glucose medium followed by 24 h treatment with metformin, cell medium was changed to unbuffered low-glucose DMEM containing the same treatment as during the previous 24 h. The plate was placed in a CO_2-free incubator at 37 °C for 1 h. According to the manufacturer's instructions, the XF24 sensor cartridge was placed in a Seahorse 24-well plate containing Seahorse XF24 calibrant (pH 7.4) (Bucher Biotec AG) and stored overnight at 37 °C without CO_2 was loaded in the Seahorse XF24 analyzer (Bucher Biotec AG). After calibration, the cell plate was loaded in the analyzer and oxygen consumption was measured over 1 h. Metformin-treated wells were compared with control untreated wells in each plate analyzed.

2.4. Glucose uptake

After treatment, 1 μCi deoxy-D-glucose, [2-^{3}H(G)] (Perkin Elmer, Schwerzenbach, Switzerland) was added to each well and allowed to incubate for 15 min. The preadipocyte-derived adipocytes were then washed with PBS and lysed in 0.1% sodium dodecyl sulfate (Sigma–Aldrich). Radioactivity was measured in a betamatic liquid scintillation counter [7]. This protocol was also applied with minor modification to mature isolated adipocytes. In brief, these cells were incubated on a shaker (100 rpm) in Krebs Ringer Buffer (pH 7.4) supplemented with 1% BSA (Sigma–Aldrich) and 1 mM glucose (Sigma–Aldrich). 1 μCi deoxy-D-glucose, [2-^{3}H(G)] was added for 15 min as described above. After the addition of dinonyl phthalate (Sigma–Aldrich), the fat layer containing mature adipocytes was collected by centrifugation and the radioactivity measured.

2.5. Glucose oxidation rate

The glucose oxidation rate was measured by the method described in the literature [8]. Preadipocytes were cultured and differentiated into adipocytes in 25 cm^2 flasks. Four hours before the end of the treatment, 2.5 μCi of [U-^{14}C]-glucose (Hartmann Analytic, Göttingen, Germany) was added to each flask and a $^{14}CO_2$-collecting device was tightly attached to the culture flask. 1 ml of 5 N sulfuric acid was added to the flask through the septum to stop metabolism and drive off all the CO_2. 30 min later, the scintillation pad saturated with 150 μl of aminoethanol (Sigma–Aldrich) was removed from the filter paper rest and the adsorbed $^{14}CO_2$ radioactivity was measured with a liquid scintillation counter.

2.6. Confocal microscopy

Preadipocytes were grown and differentiated on sterile coverslips. Adipocytes were washed and fixed on ice for 15 min with 4% PFA (Sigma–Aldrich). After blocking (PBS + 1% BSA for 15 min), cells were incubated for 30 min at RT with TRITC-concanavalin A (1:500 in PBS + 1% BSA; Lubio Science). Adipocytes were incubated overnight at 4 °C with anti-GLUT-4 polyclonal antibody (1:200 in PBS + 1% BSA; Santa Cruz Biotechnology, Santa Cruz, CA, USA). The coverslips were then washed and incubated for 1 h at RT with Alexa 488-conjugated anti-rabbit antibody (1:500 in PBS + 1% BSA) from Lubio Science and mounted in Vectashield mounting medium (Reactolab, Servion, Switzerland). Fluorescence was viewed under a confocal laser scanning Axiovert S100 microscope (Zeiss, Feldbach, Switzerland). Evaluation of GLUT-4/concanavalin A co-localization intensity was performed using LSM 510 software (Zeiss).

2.7. AMPKα1 silencing

Preadipocyte-derived adipocytes were transfected with 2 μM validated human ACCELL™ SMARTpool siRNA targeting the PRKAA1 (AMPKα1) gene using ACCELL™ delivery media (Thermo Scientific, Lafayette, CO, USA) and following the manufacturer's instructions. ACCELL™ non-targeting pool (Thermo Scientific) was used as control siRNA. Silencing was performed for 72 h and metformin treatment was added to the ACCELL™ delivery media (Thermo Scientific) for additional 24 h.

2.8. Quantitative analysis of GLUT-1, GLUT-4 and AMPK mRNA expression

RNA was isolated and 1 μg total RNA was subjected to reverse transcription-PCR. cDNA was subjected to quantitative real-time PCR analysis using the power SYBR™-Green PCR master mix (Applied Biosystems, Rotkreuz, Switzerland) and the ABI 7500 Sequence detection system [9]. Optimal sets of primers were designed for each studied gene using the "ProbeFinder" (Roche Applied Bioscience, Rotkreuz, Switzerland) website interface (http://

qpcr2.probefinder.com), including GLUT-1 sense primer, 5′-CCATTGGCTCCGGTATCGT-3′ and GLUT-1 antisense primer, 5′-TGCTCGCTCCACCACAAAC-3′; GLUT-4 sense primer, 5′-CCCCCTCAGCAGCGAGTGA-3′ and GLUT-4 antisense primer, 5′-GCACCGCCAGGACATTGTTG-3′; AMPKα1 sense primer, 5′-CAAGCTTTTCAGGCATCCTC-3′ and AMPKα1 antisense primer, 5′-CAAATAGCTCTCCTCCTGAGACA-3′; AMPKα2 sense primer, 5′-TGCAGCACCTGAAGTCATCT-3′ and AMPKα2 antisense primer, 5′-TGCCACAAAGAAGAGCATACA-3′. Hypoxanthine-guanine phosphoribosyltransferase (HPRT) primers were used as loading control HPRT sense primer, 5′-TCAGGCAGTATAATCCAAAGATGGT-3′ and HPRT antisense primer, 5′-AGTCTGGCTTATATCCAACACTTC-3′.

2.9. Adipocyte lysates

Following stimulation, adipocytes were washed with PBS. Cells were harvested in a 10 mM Tris–HCl (pH 7.4) lysis buffer containing 1% Triton-100 (Sigma–Aldrich), 0.5% Nonidet P-40, protease inhibitors cocktail (Roche Diagnostics, Rotkreuz, Switzerland) and Halt™ phosphatase inhibitor cocktail (Thermo scientific) and incubated on ice for 10 min. Cell lysates were cleared by centrifugation (10,000 × *g*, 10 min).

2.10. Plasma membrane and high-speed pellet cellular fractionation

Following stimulation, adipocytes were washed with HES buffer, scraped, homogenized and centrifuged as previously described [10]. The supernatant was further centrifuged (18,000 × *g*, 20 min). The resulting pellet represented the crude plasma membrane (PM) fractions and the supernatant was further centrifuged (30,000 × *g*, 30 min) to collect a pellet of high-density microsomes. The supernatant was cleared of remaining fat particles by filtering through a 0.45-μm filter (Millipore, Zug, Switzerland) and centrifuged (175,000 × *g*, 4 h) to obtain a high-speed pellet (HSP) also designated as the low-density microsomal fraction. This fraction was resuspended in lysis buffer and HSP lysate was obtained. The crude plasma membrane pellet was also resuspended in lysis buffer to obtain plasma membrane fraction lysate.

2.11. Western blot analysis

Protein concentrations of whole lysates, PM and HSP lysates were determined and 20 μg of protein lysates mixed in SDS sample buffer were subjected to 10% SDS-PAGE and blotted on a nitrocellulose membrane as previously described [11]. After blocking, the membrane was incubated with primary and horseradish peroxidase-conjugated antibodies. Band intensities were detected with Immun-Star HRP substrate kit (BioRad, Reinach, Switzerland) and densitometry values were calculated with the Image J software (NIH, Bethesda, MD, USA).

Primary antibodies used include rabbit polyclonal antibody to pSer-79-acetyl-CoA carboxylase (ACC), AMPKα1, AMPKα2 (Lucerna Chem, Luzern, Switzerland) pSer-473-Akt, Akt, AS160 (Bio Concept, Allschwil, Switzerland), GLUT-1, GLUT-4, β-actin (Abcam, Cambridge, UK) and pThr-642 Akt substrate of 160 kDa (AS160) (Lubio Science).

2.12. Statistical analysis

Data are presented as mean ± standard deviation (SD) from a minimum of three independent experiments. Differences between two groups were evaluated using the Mann–Whitney *U* test. For multigroup comparisons, one-way analysis of variance was performed and the Tukey's posthoc multiple comparison test was applied. Overall, a p value <0.05 was considered significant.

3. Results

3.1. Effect of metformin on cell viability and oxygen consumption in human adipocytes

In dead cells, propidium iodide (PI) can enter and becomes intercalated into the DNA, causing fluorescence to be observable. After 24 h of metformin treatment (concentrations ranging from 0.1 to 10 mM), the percentage of PI negative cells or viable cells was not significantly decreased (p = n.s.) (Fig. 1A) and the percentage of PI positive or non-viable cells was not significantly increased with increasing metformin dosage (Fig. 1B). Our preadipocyte-derived adipocyte cell population is heterogeneous. Even under optimal conditions, the differentiation efficiency is not complete. To distinguish preadipocytes from adipocytes, we stained the cells with a specific BODIPY™ dye for cellular lipid droplets permitting confirmation that metformin did not increase cytotoxicity in adipocytes (data not shown). The results obtained with PI staining were confirmed using the Live/Dead viability/cytotoxicity kit (Lubio Science) (data not shown).

In undifferentiated preadipocytes (Fig. 1C), treatment with metformin at 0.01 and 0.1 mM for 24 h tend to increase the oxygen consumption rate (OCR) (1.06 ± 0.02-fold, p = n.s. vs. basal) and decrease OCR (0.90 ± 0.02-fold, p = n.s. vs. basal), respectively. At 1 mM metformin for 24 h, OCR decreased to 0.24 ± 0.03-fold ($p < 0.001$ vs. basal). In preadipocyte-derived adipocytes (Fig. 1D), metformin at 0.01 and 0.1 mM for 24 h increased OCR 1.39 ± 0.04 and 1.36 ± 0.03-fold respectively ($p < 0.001$ vs. basal). Treatment with 1 mM metformin for 24 h did not alter the basal OCR, whereas 10 mM metformin for 24 h decreased the OCR to 0.24 ± 0.01-fold ($p < 0.001$ vs. basal).

3.2. Effect of metformin on glucose uptake in human preadipocyte-derived adipocytes and mature isolated adipocytes

Metformin treatment for 24 h induced dose-dependent increase in basal glucose uptake (Fig. 2A). Metformin concentrations from 0.001 to 0.1 mM did not significantly increase glucose uptake whereas metformin concentrations from 1 to 10 mM increased glucose uptake 2.3 ± 0.2 and 2.8 ± 0.2-fold ($p < 0.001$ vs. basal), respectively. The time-course of metformin-induced glucose uptake is shown in Fig. 2B. After 3 h, 1 mM metformin treatment was not associated with a significant increase in glucose uptake, whereas 10 mM metformin increased glucose uptake 1.6 ± 0.1-fold vs. basal, $p < 0.01$. After 24 h treatment, 1 and 10 mM metformin were both associated with an increase in cellular glucose uptake compared to basal values and to incubations for 3 h. After 48 h treatment, 1 and 10 mM metformin-induced glucose uptakes were both slightly higher compared to 24 h treatment. Based on these results, we performed further experiments using the lowest dose of metformin (i.e. 1 mM) and the shortest period of incubation (i.e. 24 h) which showed significant effects on glucose uptake. These data were also confirmed using mature adipocytes freshly isolated from patient adipose tissue (Fig. 2C), in which 24 h treatment with 1 mM metformin increased glucose uptake 2.2 ± 0.4-fold ($p < 0.05$ vs. basal).

3.3. Effect of metformin on GLUT-1 and GLUT-4 glucose transporters

Metformin-induced glucose uptake was inhibited by phloretin, an inhibitor of glucose transporters (data not shown). GLUT-1 mRNA expression was not altered by metformin (Fig. 3A). GLUT-4 mRNA expression was increased 4.2 ± 0.5-fold ($p < 0.01$ vs. basal) (Fig. 3B). Similarly, after metformin treatment, the protein level of GLUT-1 was not altered (Fig. 3C and E) while GLUT-4 protein content was increased (up to 2.6-fold, $p < 0.01$ vs. basal, Fig. 3D and F).

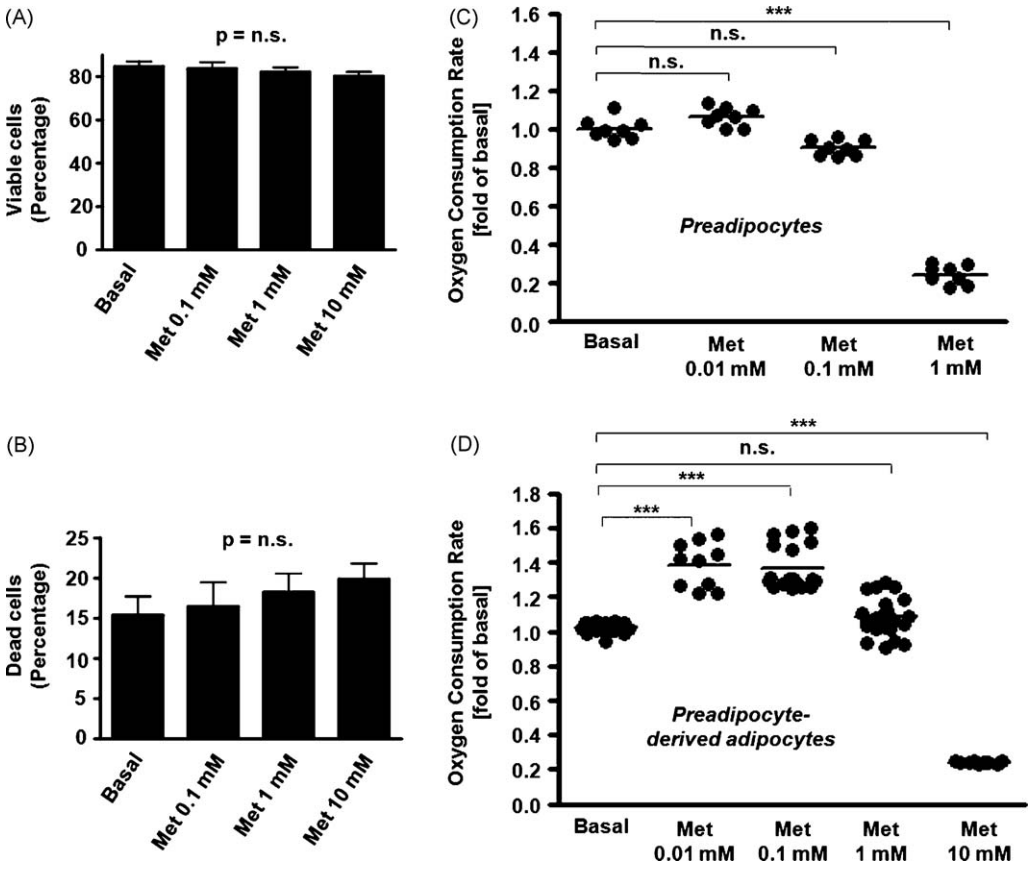

Fig. 1. Effect of metformin on cell viability and respiration. Preadipocyte-derived adipocytes were treated for 24 h with metformin (Met) with concentrations ranging from 0.01 to 10 mM. The percentage of viable cells (A) and dead cells (B) was measured by flow cytometry using propidium iodide staining. Data are presented as percentage of the total cell number showing the mean ± SD of three independent experiments (p = n.s., not significant). The cellular oxygen consumption rate was determined using the Seahorse device in preadipocytes before differentiation (C) and in preadipocyte-derived adipocytes after 14 days of differentiation (D). Data are presented as fold of basal (OCR mean obtained from untreated cells in preadipocytes and preadipocyte-derived adipocytes, respectively) showing the mean ± SD of three independent experiments, each performed with a minimum of three cell culture wells per treatment and analyzed for one hour (***$p < 0.001$ vs. basal; p = n.s., not significant).

Confocal microscopy of immunocytochemically stained cells showed co-localization (yellow color) of GLUT-4 protein (green immunostaining) with labeled concanavalin A (red staining) (Fig. 4A). Concanavalin A binds to glycosylated residues on cell surface proteins and localized the PM in fixed, non-permeabilized adipocytes. The co-localization signal of GLUT-4 with the PM was quantified by determining the size of the respective areas of co-localization in the microscopic fields (Fig. 4B). This technique showed an increase in the co-localization area from $310 \pm 20\ \mu m^2$ in the basal state to $530 \pm 30\ \mu m^2$ ($p < 0.001$ vs. basal) and $460 \pm 30\ \mu m^2$ ($p < 0.01$ vs. basal) after insulin and metformin stimulation, respectively. Co-treatment with insulin and metformin was the most potent inducer of this signal ($610 \pm 40\ \mu m^2$, $p < 0.001$ vs. basal or $p < 0.05$ vs. insulin).

To validate these results, we conducted subcellular fractionation analysis. GLUT-1 protein content at the plasma membrane was very low and was not or only very slightly altered by insulin and/or metformin treatments (Fig. 4C). Insulin stimulation of human adipocytes leads to translocation of GLUT-4 from its intracellular storage vesicles (HSP fraction) to the PM. In metformin-treated cells, GLUT-4 protein levels increased in both HSP and PM fractions and insulin-induced translocation of GLUT-4 to the PM was observed. Quantitative analysis of PM immunoblots (Fig. 4D) showed that insulin increased the GLUT-4 protein content in the PM fraction 1.3 ± 0.1-fold ($p < 0.05$ vs. basal). Metformin similarly increased GLUT-4 content in the PM (1.3 ± 0.1-fold vs. basal, $p < 0.05$), and co-treatment with insulin strongly enhanced GLUT-4 content in the PM (1.8 ± 0.1-fold, $p < 0.001$ vs. basal or vs. insulin).

3.4. Effect of metformin on Akt signaling pathway

Phosphorylation of Akt at Ser-473 was increased by insulin demonstrating that insulin activates Akt (Fig. 5A). Metformin neither increased alone Akt phosphorylation nor altered insulin-induced Akt phosphorylation. The total Akt protein content was similar in basal, insulin- and metformin-treated adipocytes. Insulin induced a significant 2.9 ± 0.1-fold ($p < 0.01$ vs. basal) increase in the pThr-642 AS160 signal, which is a crucial step in insulin-induced GLUT-4 translocation (Fig. 5B). It is noteworthy that metformin did not alter either basal or insulin-induced AS160 phosphorylation (p = n.s.).

3.5. Effect of AMPKα1 silencing on metformin-increased GLUT-4 level and metformin-induced glucose uptake

Phosphorylation at Ser-79 of acetyl-CoA carboxylase (ACC), a surrogate marker for AMPK activity, was evaluated by immunoblotting. In preadipocytes, ACC phosphorylation was not detectable. The ACC phosphorylation signal appeared after 7 days of differentiation and its intensity was further increased at 14 days of differentiation (Fig. 6A). In concert with decreased β-actin loading control due to morphological changes during adipose differentiation [12], GLUT-4, AMPKα1 and AMPKα2 protein contents

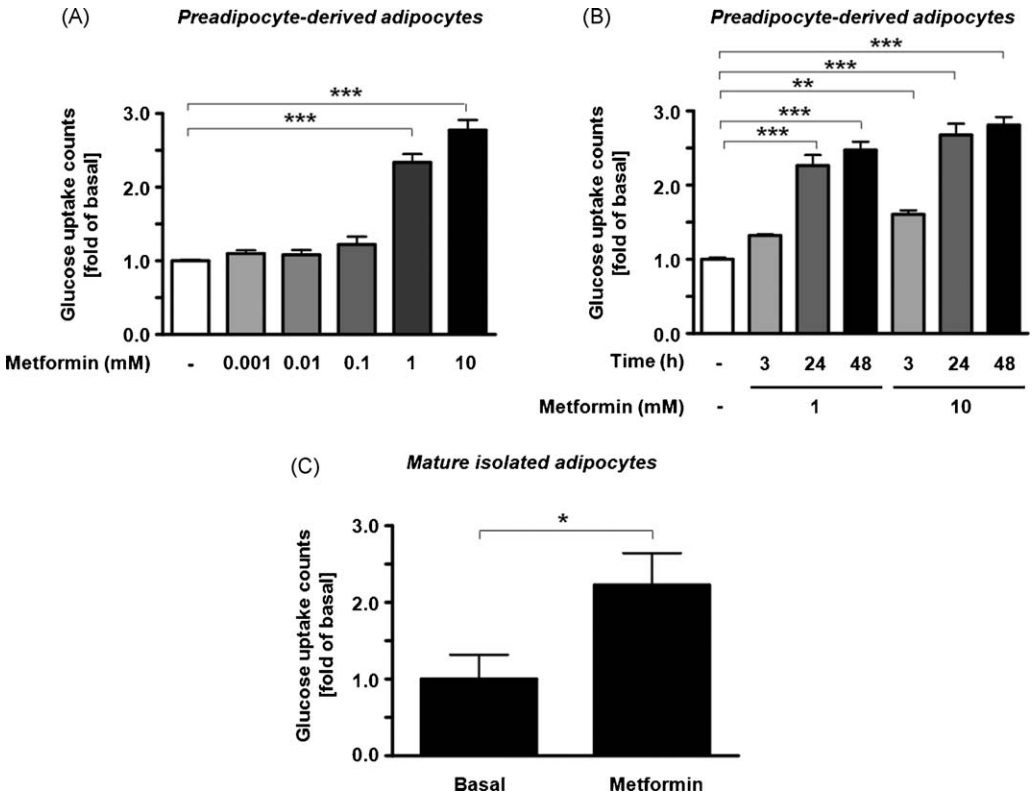

Fig. 2. Effect of metformin on glucose uptake. Glucose uptake was determined using radioactively labeled glucose after the indicated treatment of the cells. (A) Preadipocyte-derived adipocytes were treated for 24 h with metformin from 0.001 to 10 mM. Data are presented as fold of basal and are reported as the mean ± SD of three independent experiments (***$p < 0.001$ vs. basal). (B) Preadipocyte-derived adipocytes were treated with 1 or 10 mM metformin for 3 to 48 h. Data are presented as fold of basal and are reported as the mean ± SD of three independent experiments (**$p < 0.01$ vs. basal; ***$p < 0.001$ vs. basal). C. Mature isolated adipocytes were treated for 24 h with 1 mM metformin. Data given as fold of basal are the mean ± SD of three independent experiments using primary adipocytes from 2 non-obese and 1 obese patients (*$p < 0.05$ vs. basal).

increased with differentiation. However, the AMPKα2 signal was weak in comparison with AMPKα1 although the film was exposed for longer periods of time to detect AMPKα2. Consistent with the protein levels, AMPKα1 mRNA expression was 5-fold higher than AMPKα2 (data not shown).

We then silenced the AMPKα1 isoform in preadipocyte-derived adipocytes differentiated for 14 days. In control siRNA treated cells, the mRNA expression of AMPKα1 and AMPKα2 was increased upon treatment with metformin (Fig. 6B). Using a siRNA pool specifically targeting AMPKα1, AMPKα1 mRNA expression was decreased to 0.28 ± 0.03 and 0.32 ± 0.05-fold ($p < 0.001$ vs. control siRNA) and AMPKα1 protein content was decreased to 0.50 ± 0.08 and 0.45 ± 0.09-fold ($p < 0.001$ vs. control siRNA) in untreated and metformin-treated cells respectively (Fig. 6C and D). In contrast, AMPKα2 protein level and mRNA expression were not altered (p = n.s.) by AMPKα1 silencing. Metformin did not significantly increase AMPKα1 protein content in control siRNA treated cells (Fig. 6D) but did increase phosphorylation of ACC at Ser-79 to 2.07 ± 0.12-fold ($p < 0.001$ vs. basal control siRNA) (Fig. 6C and E). Therefore, metformin activated AMPK in our human adipocytes. AMPKα1 silencing reduced both basal and metformin-induced ACC phosphorylation to 0.68 ± 0.05 and 1.43 ± 0.15-fold ($p < 0.001$ vs. control siRNA), respectively. Interestingly, GLUT-4 protein content in the cell lysate and in the plasma membrane fraction was decreased upon AMPKα1 silencing in both untreated and metformin-treated cells (Fig. 6C). In control siRNA treated cells, metformin induced glucose uptake 1.9 ± 0.1-fold ($p < 0.001$ vs. basal) while in AMPKα1 silenced cells, metformin-induced glucose uptake was only increased 1.3 ± 0.1-fold ($p < 0.001$ vs. metformin control siRNA) (Fig. 6F).

3.6. Effect of metformin on glucose oxidation

Upon metformin stimulation, the CO_2 recovery (Fig. 7), which reflects the glucose oxidation rate, increased 2.2 ± 0.5-fold ($p < 0.05$ vs. basal).

4. Discussion

Metformin at the dose of 1 mM increased glucose uptake in human adipocytes without altering cell viability or impairing cell respiration. Metformin induced glucose uptake independently of the classical Akt/AS160 pathway. Metformin increased intracellular GLUT-4 mRNA expression and subsequently increased protein content in the GLUT-4 storage vesicles and in the plasma membrane. AMPKα1 silencing suppressed metformin-induced GLUT-4 expression and glucose uptake, demonstrating that activation of AMPK is involved in the mechanism of metformin effects on glucose metabolism. Additionally, metformin induced glucose oxidation in human adipocytes.

In rat adipocytes, metformin blocks down-regulation of cell surface GLUT-4 induced by chronic insulin treatment [13] and directly potentiates the insulin-induced GLUT-4 translocation [14]. In our human adipocytes, insulin (100 nM, 20 min) and metformin (1 mM, 24 h) showed additive effects on glucose uptake in subcutaneous preadipocyte-derived adipocytes independently of BMI, gender and age of the patients [7], consistent with distinct signaling pathways triggering these effects. Herein we demonstrate that metformin-induced glucose uptake is independent of the classical "Akt/AS160" insulin signaling pathway in human adipocytes.

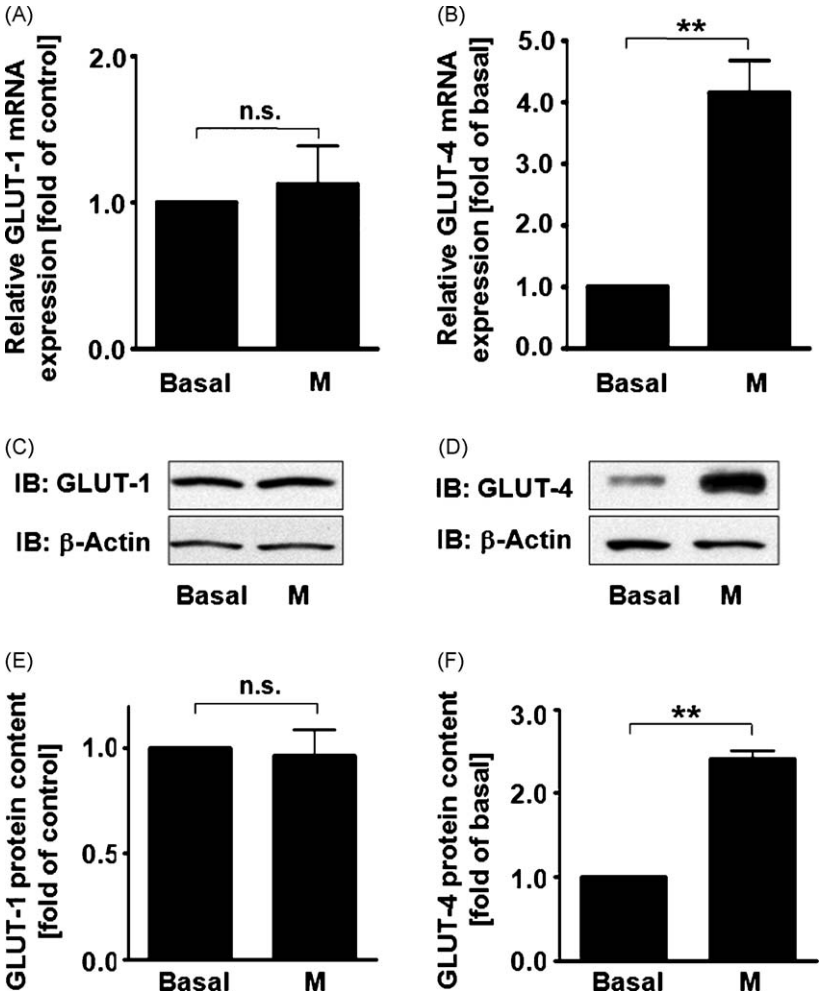

Fig. 3. Effect of metformin on GLUT-1 and GLUT-4 mRNA expression and protein content. Preadipocyte-derived adipocytes were treated for 24 h with 1 mM metformin (M). mRNA expression of glucose transporters was analyzed by quantitative real-time PCR using GLUT-1 primers (A) or GLUT-4 primers (B). HPRT was used as an internal control to correct loading variation. Data are presented as fold of basal and are reported (A and B) as means ± SD of three independent experiments ($^{**}p < 0.01$ vs. basal; n.s. = not significant vs. basal). Immunoblots showing the protein contents of GLUT-1 (C) and GLUT-4 (D). β-Actin was used as a loading control. Quantitative analysis of GLUT-1 (E) and GLUT-4 (F) protein levels given as fold of basal and corrected for potential loading variations using β-actin. Data (E and F) are means ± SD of three independent experiments ($^{**}p < 0.01$ vs. basal).

Exposure of cultured human myotubes to metformin increased mRNA expression of GLUT-4 [15] and metformin stimulates glucose transport via a decrease in GLUT-4 endocytosis in an AMPK-dependent manner in cardiac myocytes [16]. Activation of AMPK by the AMP-mimetic 5-aminoimidazole-4-carboxamide ribonucleoside (AICAR) stimulates GLUT-4 expression [17,18], its translocation to the cell membrane and subsequent glucose uptake in rat skeletal muscle [19–21]. The effects of AMPK on GLUT-4 in skeletal and cardiac muscle are responsible for the beneficial action of AMPK activators on glucose uptake. AICAR also increased GLUT-4 mRNA expression and protein content in our human adipocytes (data not shown). Using RNA interference, we demonstrated that AMPKα1 is required in metformin-induced GLUT-4 expression and accumulation in the plasma membrane, and that AMPKα1 is involved in metformin-induced glucose uptake. In 3T3-L1 adipocytes, AMPKα2 is predominantly expressed [22], while AMPKα1 is the prevalent subunit in rat adipocytes [23,24]. As in rat adipocytes, AMPKα2 expression, at both the mRNA and protein levels, was lower than AMPKα1, suggesting that AMPKα2 is only weakly expressed in human adipocytes. AMPKα2 does not compensate for the AMPKα1 silencing-induced decreases in AMPKα mRNA and protein expression, and the decrease in ACC phosphorylation at Ser-79. This may explain the crucial role of AMPKα1 in the effect of metformin on GLUT-4 expression and function. While significant activity of AMPK is still observed after AMPKα1 silencing, this is likely due to only partial knockdown and the residual AMPKα1 protein present in the cells. However, these results do not rule out an effect of AMPKα2 on glucose uptake, as metformin is an efficient inducer of both subunits [25].

It has been established that metformin inhibits the enzymatic activity of complex I of the respiratory chain, thereby impairing both mitochondrial function and cell respiration in skeletal muscle and liver [26,27]. The activation of AMPK by metformin might therefore be in response to complex 1 inhibition. It is also known that inhibition of the respiratory chain can be associated with upregulation of the expression of glucose transporters and glycolytic enzymes leading to glycolytic glucose utilization. Thus, it could be predicted that the inhibition of respiratory chain by metformin would elicit an increase in glucose transport and glycolysis [28]. Such an increase in glucose transport associated with a decrease of glucose oxidation was observed in isolated muscle and proposed to be as a consequence of impaired cell respiration [29]. In our human adipocytes, using similar

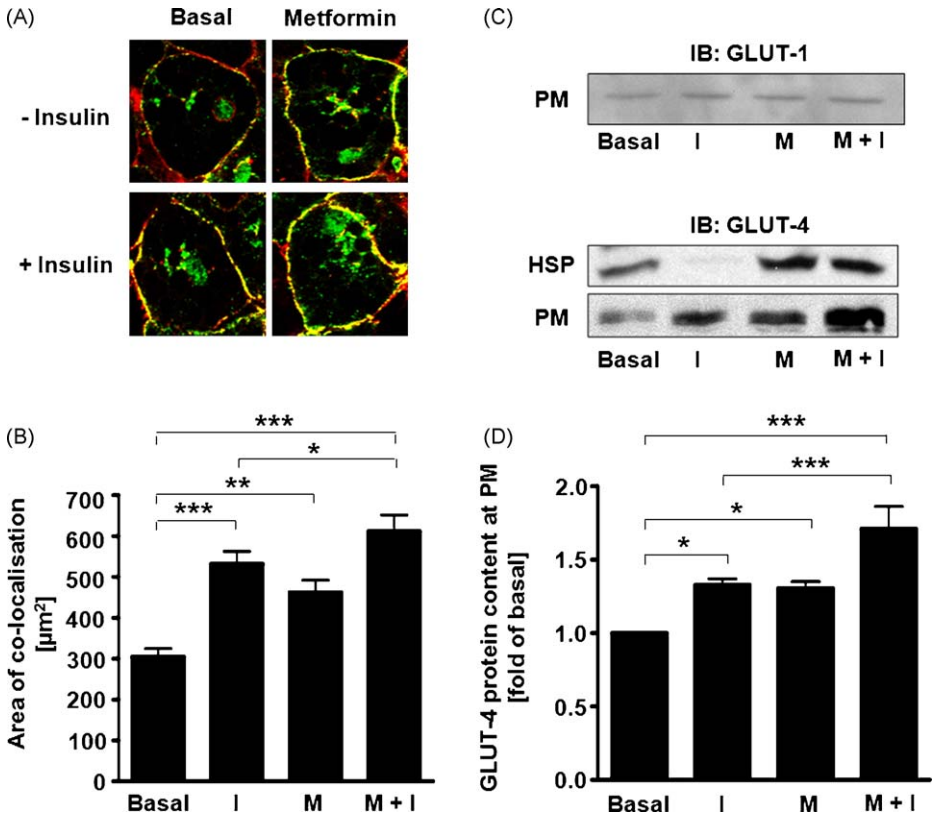

Fig. 4. Effect of metformin on GLUT-4 localization. Preadipocyte-derived adipocytes were left untreated or treated for 24 h with 1 mM metformin (M) followed or not by 100 nM insulin (+I) stimulation for 20 min. (A) Co-localization (yellow color) resulting from association of GLUT-4 protein (green immunostaining) with the labeled plasma membrane (red fluorescence representing binding of TIRTC-labeled concanavalin A to glycosylated residues on the surface of intact cells). (B) Quantitative analysis of the co-localization signal using the confocal microscope software LSM510 showed similar results as described for plasma membrane immunoblot analysis. Data represent means ± SD of the co-localization area (in μm^2) for ten fields from three independent experiments. (*$p < 0.05$ vs. insulin; **$p < 0.01$ vs. basal; ***$p < 0.001$ vs. basal). (C) High-speed pellet (HSP) and plasma membrane (PM) fractionation was performed and the respective lysates were subjected to immunoblotting that detected the GLUT-1 and GLUT-4 protein content. (D) Quantification of GLUT-4 protein levels in the plasma membrane are presented as fold of basal and are from three independent experiments (*$p < 0.05$ vs. basal; ***$p < 0.001$ vs. basal or vs. insulin).

concentrations and time of exposure, metformin increased both glucose uptake and glucose oxidation, which is in agreement with previous work performed in C3Hl0T1/2-derived adipocytes [30]. Although 24 h treatment with 1 mM metformin did not impair cell respiration, oxygen consumption was dramatically impaired after 24 h treatment with 10 mM metformin. Both metformin doses were, however, associated with a similar increase in cellular glucose uptake in preadipocyte-derived adipocytes. Together, these findings rule out mitochondrial dysfunction as a major mechanism for the observed effects of metformin in our human adipocytes. This also suggests that the effect of metformin on AMPK is independent of the effect on the mitochondrial chain. Intriguing data showed an increase in the OCR after 24 h treatment with 0.01 and 0.1 mM metformin in preadipocyte-derived adipocytes. This was not observed in the preadipocytes. Treatment for 24 h with 1 mM metformin did not alter the OCR in differentiated preadipocyte-derived adipocytes and dramatically decreased OCR in preadipocytes. Therefore, the OCR-lowering effect of metformin (1 mM, 24 h) in preadipocytes might counterbalance the OCR increase in mature and metabolically active adipocytes, leading to the unchanged OCR observed in our heterogeneous, and not completely differentiated, preadipocyte-derived adipocyte cell population. In addition, the OCR varied from 0.91- to 1.28-fold in our preadipocyte-derived adipocytes treated with 1 mM metformin for 24 h. This variation might be caused by varying differentiation efficiencies in the primary preadipocytes used in each experiment. A tendency toward lower OCR in less differentiated cell culture seemed to be present, but this needs to be further investigated. The use of primary mature adipocytes isolated from patient adipose tissue would have been more relevant. However, OCR experiments cannot be performed in floating adipocytes due to technical limitations.

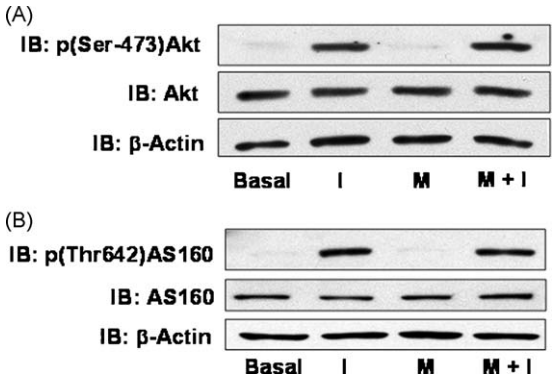

Fig. 5. Effect of metformin on Akt signaling pathway. Preadipocyte-derived adipocytes were left untreated or treated for 24 h with 1 mM metformin (M) followed or not by 100 nM insulin (+I) stimulation for 20 min. (A) Immunoblots (IB) showing the phosphorylation status at Ser-473 and the protein content of Akt. β-Actin was used as loading control. (B) Immunoblots showing the phosphorylation (p) status at Thr-642 and the protein content of AS160. β-Actin was used as loading control.

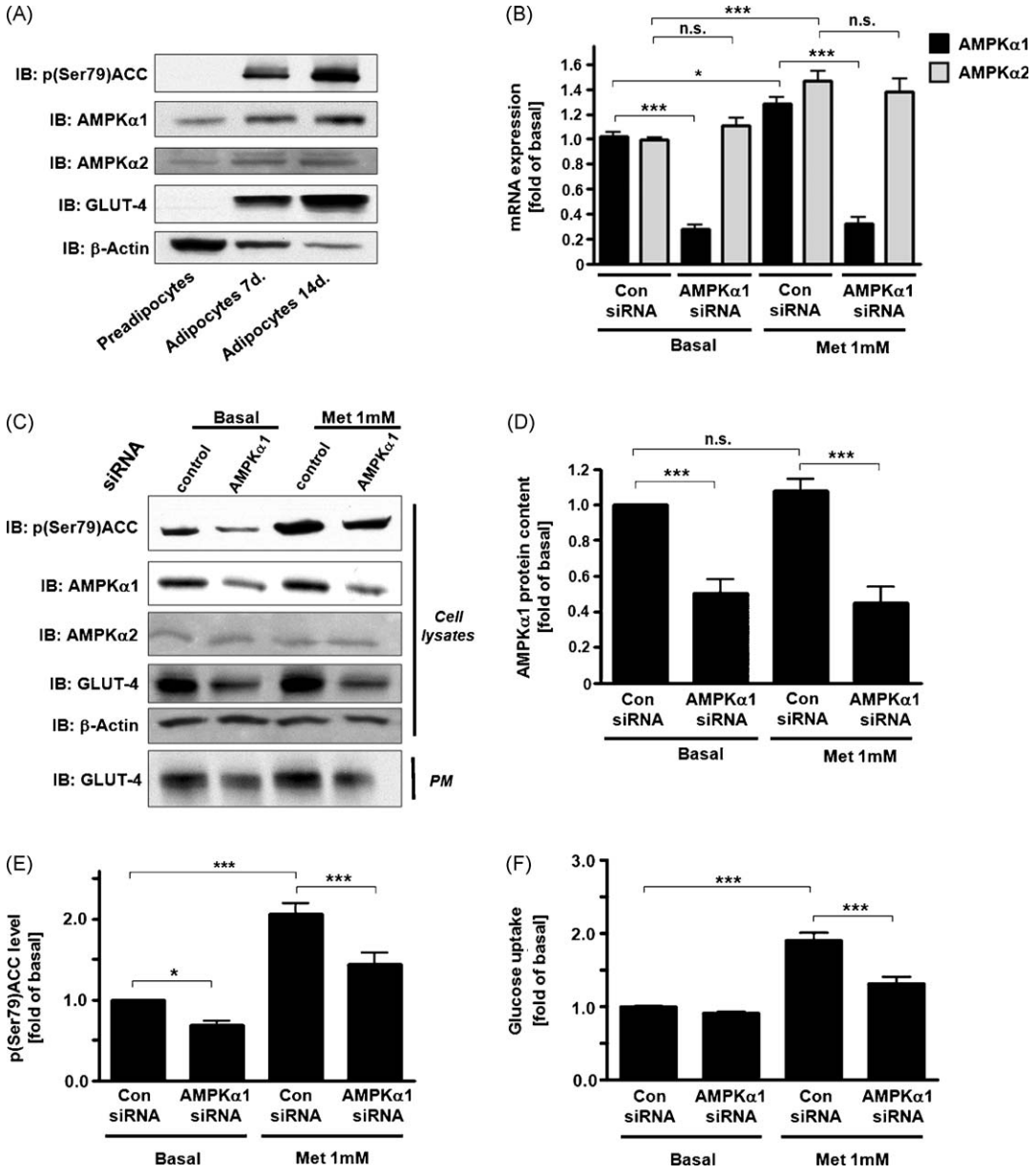

Fig. 6. Effect of AMPKα1 silencing on metformin-increased GLUT-4 level and -induced glucose uptake. Preadipocytes and preadipocyte-derived adipocytes after 7 days (7 d) and 14 days (14 d) of differentiation were harvested. Preadipocyte-derived adipocytes after 14 days of differentiation were transfected for 72 h with a control of non-targeting siRNA pool (Con siRNA) or siRNA pool specifically targeting AMPKα1 (AMPKα1 siRNA) and treated for 24 h with 1 mM metformin (Met). (A) Immunoblots (IB) showing the phosphorylation status at Ser-79 of acetyl-CoA carboxylase (ACC) and the protein content of GLUT-4, AMPKα1 and AMPKα2 isoforms. β-Actin was used as loading control. (B) mRNA expression of AMPKα1 and AMPKα2 isoforms was analyzed by quantitative real-time PCR. HPRT was used as an internal control to correct for loading variation. Data are presented as fold of basal of control siRNA and are reported as means ± SD of three independent experiments (*$p < 0.05$ vs. basal control siRNA; ***$p < 0.001$ vs. control siRNA; n.s. = not significant vs. basal). (C) Immunoblots showing the phosphorylation status at Ser-79 of acetyl-CoA carboxylase (ACC), the protein content of AMPKα1 and AMPKα2 isoforms and the protein content of GLUT-4 in total cell lysates and plasma membrane (PM) fractions. β-actin was used as loading control. (D) Quantitative analysis of AMPKα1 protein content given as fold of basal control siRNA and corrected for potential loading variations using β-actin. Data are means ± SD of three independent experiments (***$p < 0.001$ vs. control siRNA; n.s. = not significant vs. basal control siRNA). (E) Quantitative analysis of phosphorylation status of ACC at Ser-79 given as fold of basal control siRNA and corrected for potential loading variations using β-actin. Data are means ± SD of three independent experiments (*$p < 0.05$ vs. basal control siRNA; ***$p < 0.001$ vs. control siRNA). (F) Glucose uptake data given as fold of basal are the mean ± SD of three independent experiments (***$p < 0.001$ vs. control siRNA).

Interestingly, GLUT-4 concentrations are reduced in adipocytes from obese subjects and from patients with impaired glucose tolerance or type 2 diabetes [31]. In insulin-resistant patients with polycystic ovary syndrome, metformin therapy markedly improved GLUT-4 mRNA expression in adipose tissue [32]. However, it should be noted that these results are at variance with a previous study [33] that reports unchanged adipocyte content of GLUT-4 in type 2 diabetic subjects treated with metformin. These contradictory findings may be the result of different experimental designs and measurements. Indeed, patients known to be unresponsive to the sulfonylurea glyburide were used in the study which reported no change in adipocyte content of GLUT-4. Glipizide, another sulfonylurea, upregulates GLUT-4 [34], so selecting patients unresponsive to glyburide may also mean that those patients are inherently unable to upregulate GLUT-4 by metformin.

In conclusion, metformin-increased GLUT-4 production in human adipocytes could counteract the deleterious loss of this glucose transporter in insulin-resistant adipose tissues. Our data

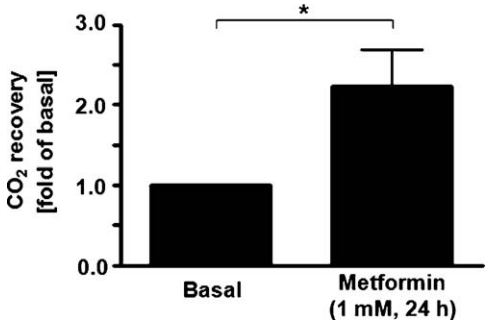

Fig. 7. Effect of metformin on glucose oxidation. Preadipocyte-derived adipocytes were treated for 24 h with 1 mM metformin including 4 h in the presence of $^{14}C(U)$-glucose. Using a $^{14}CO_2$-collecting device, CO_2 recovery was measured by a liquid scintillation counter. Data given as fold of the basal rate are the mean ± SD of three independent experiments ($^*p < 0.001$ vs. basal).

also demonstrate that treatment with 1 mM metformin for 24 h increases glucose uptake via an AMPKα1 pathway, and does not detrimentally affect cell respiration or viability in mature adipocytes.

Conflict of interest statement

The authors state no conflict or duality of interest in regards to this work.

Acknowledgements

This study was supported by grants from the University of Basel (Forschungsfonds-Förderung für Nachwuchsforschende der Universität Basel) and the Stiftung der Diabetes-Gesellschaft Region Basel to Jean Grisouard, the Novartis Stiftung für Medizinisch-Biologische Forschung and the Swiss National Research Foundation (PP00P3_123346/1) to Mirjam Christ-Crain and Sanofi-Aventis to Beat Müller.

We thank Kaethi Dembinski (Department of Biomedicine, University Hospital Basel) for her outstanding technical assistance regarding adipocytes cell culture, glucose uptake measurements and quantification of mRNA expression by real-time PCR.

Additional thanks to Dr. Anja Zahno (Department of Biomedicine, University Hospital Basel), Peter Mullen (Department of Biomedicine, University Hospital Basel), Dr. Peter Lindinger (Department of Biomedicine, University Hospital Basel), Estelle Hirzel (Department of Biomedicine, University Hospital Basel) and Dr. Karin Brecht (Department of Biomedicine, University Hospital Basel) for their expertise with oxygen consumption measurement and mitochondrial respiration and to Beat Erne (Department of Biomedicine, University Hospital Basel) for his valuable technical assistance regarding confocal microscopy.

Special thanks to Dr. Stefan Wueest (University Children's Hospital Zürich) and Prof. Daniel Konrad (University Children's Hospital Zürich) for their protocol to measure glucose uptake in isolated mature adipocytes, to Verena Jäggin (Department of Biomedicine, University Hospital Basel) for her help with flow cytometry and to Beatrice Tonnarelli (Department of Biomedicine, University Hospital Basel) for providing us with the cell viability kit.

References

[1] Bailey CJ, Turner RC. Metformin. N Engl J Med 1996;334:574–9.
[2] Witters LA. The blooming of the French lilac. J Clin Invest 2001;108:1105–7.
[3] Zhou G, Myers R, Li Y, Chen Y, Shen X, Fenyk-Melody J, et al. Role of AMP-activated protein kinase in mechanism of metformin action. J Clin Invest 2001;108:1167–74.
[4] Shaw RJ, Lamia KA, Vasquez D, Koo SH, Bardeesy N, Depinho RA, et al. The kinase LKB1 mediates glucose homeostasis in liver and therapeutic effects of metformin. Science 2005;310:1642–6.
[5] Watson RT, Kanzaki M, Pessin JE. Regulated membrane trafficking of the insulin-responsive glucose transporter 4 in adipocytes. Endocr Rev 2004;25:177–204.
[6] Khan AH, Pessin JE. Insulin regulation of glucose uptake: a complex interplay of intracellular signaling pathways. Diabetologia 2002;45:1475–83.
[7] Fischer M, Timper K, Radimerski T, Dembinski K, Frey DM, Zulewski H, et al. Metformin induces glucose uptake in human preadipocyte-derived adipocytes from various fat depots. Diabetes Obes Metab 2010;12:356–9.
[8] Krieg RC, Liotta LA, Petricoin III EF, Herrmann PC. Trapping radioactive carbon dioxide during cellular metabolic assays under standard culture conditions: description of a unique gas-capturing device. J Biochem Biophys Methods 2004;58:119–24.
[9] Linscheid P, Seboek D, Zulewski H, Keller U, Muller B. Autocrine/paracrine role of inflammation-mediated calcitonin gene-related peptide and adrenomedullin expression in human adipose tissue. Endocrinology 2005;146:2699–708.
[10] Whitehead JP, Molero JC, Clark S, Martin S, Meneilly G, James DE. The role of Ca2+ in insulin-stimulated glucose transport in 3T3-L1 cells. J Biol Chem 2001;276:27816–24.
[11] Grisouard J, Medunjanin S, Hermani A, Shukla A, Mayer D. Glycogen synthase kinase 3 protects estrogen receptor alpha from proteasomal degradation and is required for full transcriptional activity of the receptor. Mol Endocrinol 2007;21:2427–39.
[12] Spiegelman B, Farmer SR. Decreases in tubulin and actin gene expression prior to morphological differentiation of 3T3 adipocytes. Cell 1982;29:53–60.
[13] Kozka IJ, Holman GD. Metformin blocks downregulation of cell surface GLUT4 caused by chronic insulin treatment of rat adipocytes. Diabetes 1993;42:1159–65.
[14] Matthaei S, Hamann A, Klein HH, Benecke H, Kreymann G, Flier JS, et al. Association of metformin's effect to increase insulin-stimulated glucose transport with potentiation of insulin-induced translocation of glucose transporters from intracellular pool to plasma membrane in rat adipocytes. Diabetes 1991;40:850–7.
[15] Al-Khalili L, Forsgren M, Kannisto K, Zierath JR, Lonnqvist F, Krook A. Enhanced insulin-stimulated glycogen synthesis in response to insulin, metformin or rosiglitazone is associated with increased mRNA expression of GLUT4 and peroxisomal proliferator activator receptor gamma co-activator 1. Diabetologia 2005;48:1173–9.
[16] Yang J, Holman GD. Long-term metformin treatment stimulates cardiomyocyte glucose transport through an AMP-activated protein kinase-dependent reduction in GLUT4 endocytosis. Endocrinology 2006;147:2728–36.
[17] Holmes BF, Kurth-Kraczek E, Winder WW. Chronic activation of 5′-AMP activated protein kinase increases GLUT-4, hexokinase, and glycogen in muscle. J Appl Physiol 1999;87:1990–5.
[18] Holmes BF, Sparling DP, Olson AL, Winder WW, Dohm GL. Regulation of muscle GLUT4 enhancer factor and myocyte enhancer factor 2 by AMP-activated protein kinase. Am J Physiol Endocrinol Metab 2005;289:E1071–6.
[19] Kurth-Kraczek EJ, Hirshman MF, Goodyear LJ, Winder WW. 5′ AMP-activated protein kinase activation causes GLUT4 translocation in skeletal muscle. Diabetes 1999;48:1667–71.
[20] Buhl ES, Jessen N, Schmitz O, Pedersen SB, Pedersen O, Holman GD, et al. Chronic treatment with 5-aminoimidazole-4-carboxamide ribofuranoside increases insulin-stimulated glucose uptake and GLUT4 translocation in rat skeletal muscles in a fiber type-specific manner. Diabetes 2001;50:12–7.
[21] Yamaguchi S, Katahira H, Ozawa S, Nakamichi Y, Tanaka T, Shimoyama T, et al. Activators of AMP-activated protein kinase enhance GLUT4 translocation and its glucose transport activity in 3T3-L1 adipocytes. Am J Physiol Endocrinol Metab 2005;289:E643–649.
[22] Salt IP, Connell JM, Gould GW. 5-aminoimidazole-4-carboxamide ribonucleoside (AICAR) inhibits insulin-stimulated glucose transport in 3T3-L1 adipocytes. Diabetes 2000;49:1649–56.
[23] Kola B, Grossman AB, Korbonits M. The role of AMP-activated protein kinase in obesity. Front Horm Res 2008;36:198–211.
[24] Daval M, Diot-Dupuy F, Bazin R, Hainault I, Viollet B, Vaulont S, et al. Anti-lipolytic action of AMP-activated protein kinase in rodent adipocytes. J Biol Chem 2005;280:25250–7.
[25] Fryer LGD, Foufelle F, Barnes K, Baldwin SA, Woods A, Carling D. Characterization of the role of the AMP-activated protein kinase in the stimulation of glucose transport in skeletal muscle cells. Biochem J 2002;363:167–74.
[26] El-Mir MY, Nogueira V, Fontaine E, Avéret N, Rigoulet M, Leverve X. Dimethylbiguanide inhibits cell respiration via an indirect effect targeted on the respiratory chain complex I. J Biol Chem 2000;275:223–8.
[27] Detaille D, Guigas B, Leverve X, Wiernsperger N, Devos P. Obligatory role of membrane events in the regulatory effect of metformin on the respiratory chain function. Biochem Pharmacol 2002;63:1259–72.
[28] Owen MR, Doran E, Halestrap AP. Evidence that metformin exerts its anti-diabetic effects through inhibition of complex 1 of the mitochondrial respiratory chain. Biochem J 2000;348:607–14.
[29] Brunmair B, Staniek K, Gras F, Scharf N, Althaym A, Clara R, et al. Thiazolidinediones, like metformin, inhibit respiratory complex I. Diabetes 2004;53:1052–9.
[30] Lenhard JM, Kliewer SA, Paulik MA, Plunket KD, Lehmann JM, Weiel JE. Effects of troglitazone and metformin on glucose and lipid metabolism. Biochem Pharmacol 1997;54:801–8.

[31] Shepherd PR, Kahn BB. Glucose transporters and insulin action – implications for insulin resistance and diabetes mellitus. N Engl J Med 1999;341:248–57.
[32] Jensterle M, Janez A, Mlinar B, Marc J, Prezelj J, Pfeifer M. Impact of metformin and rosiglitazone treatment on glucose transporter 4 mRNA expression in women with polycystic ovary syndrome. Eur J Endocrinol 2008;158:793–801.
[33] Ciaraldi TP, Kong AP, Chu NV, Kim DD, Baxi S, Loviscach M, et al. Regulation of glucose transport and insulin signaling by troglitazone or metformin in adipose tissue of type 2 diabetic subjects. Diabetes 2002;51:30–6.
[34] Schmitz O, Lund S, Bak JF, Orskov L, Andersen PH, Møller N, et al. Effects of glipizide on glucose metabolism and muscle content of the insulin-regulatable glucose transporter (GLUT-4) and glycogen synthase activity during hyperglycemia in type 2 diabetic patients. Acta Diabetol 1994;31:31–6.